

Design and Analysis of the Hexagonal-Shaped Antenna with Multi-Band Feature for WLAN, WiMAX, and LTE Applications

Alaa M. Abdulhussein^{1a*}, Wasan Abd Al-Rahman Khalaf^{2b}, Nooralhuda M. Abdulhussein^{3c}, Eman Ibrahim Awad^{4d}, Ali Mohammed Ali^{4e}

¹Department of Scholarships and Cultural Relations, University of Kerbala, Kerbala, Iraq

²Department of Physics, College of Science for Women, University of Baghdad, Baghdad, Iraq

³Colleg of Pharmacy, Al-Zahraa University for Women, Kerbala, Iraq

⁴Department of Medical Physics, College of Applied Medical Science, University of Kerbala, Kerbala, Iraq

^bE-mail: wasanabda@gmail.com, ^cE-mail: nooralhuda.mohammed@alzahraa.edu.iq

^dE-mail: eman.ibrahim@uokerbala.edu.iq, ^eE-mail: ali.h.mohammedali@uokerbala.edu.iq

^{a*}Corresponding author: alaa.m.abdulhussein@uokerbala.edu.iq

Abstract

Developing and researching antenna designs is analogous to excavating in an undiscovered mine. This paper proposes a multi-band antenna with a new hexagonal ring shape, theoretically designed, developed, and analyzed using a CST before being manufactured. The antenna has undergone six changes to provide the best performance. The results of the surface current distribution and the electric field distribution on the surface of the hexagonal patch were theoretically analyzed and studied. The sequential approach taken to determine the most effective design is logical, and prevents deviation from the work direction. After comparing the six theoretical results, the fifth model proved to be the best for making a prototype. Measured results represent that the proposed antenna can operate well in three bands with a return loss of -11.24 dB at 2.9 GHz, -25.99 dB at 4.9 GHz, and -21.26 dB at 5.4 GHz. This type of antenna belongs to various wireless communication systems, including 2G, 3G, 4G, and 5G.

Article Info.

Keywords:

Planar antennas, Communication, Hexagonal Shape, Multi-Band, CNC method.

Article history:

Received: Mar. 15, 2023

Accepted: May. 04, 2023

Published: Jun. 01, 2023

1. Introduction

The 19th century saw the creation of the first antennas for wireless communication. These were straightforward wire antennas for signal transmission and reception. In 1887, Heinrich Hertz invented the first simple dipole antenna comprised of two metal rods [1]. Day-by-day wireless communication technology is increasing rapidly, and amazing growth has been observed in this system and its applications [2]. Generally, the antenna is used as a transducer, which is employed to receive or transmit electromagnetic (EM) waves. Recent technology has put a special status on consistency and small size, internetworking across the globe, and making technology provide all-time wireless communication, which should be noise-free, cost-effective, and robust [3, 4]. Microstrip patch antennas (MPAs) are the best choice for wireless communication equipment. The low-profile, low cost and low volume are the main advantages of this antenna. It can be mounted on missiles, rockets, and satellites without major adjustments [5].

With the fast growth of new communication systems, such as radio-frequency identification (RFID), worldwide interoperability for microwave access (WiMAX), and wireless local area network (WLAN) have been mainly employed as key components [6]. There is a good demand for antennas with the capability of providing a great impedance bandwidth (BW) and planar geometry for WiMAX, WLAN, and RFID applications in numerous bands, such as 2.3/2.5/3.3/5/5.5 GHz and 2.4/3.6/4.9-5.9 GHz, respectively [7]. The feed lines and patches usually are photo etched on the dielectric substrate. A triangular, square, thin strip (dipole), rectangular, elliptical, circular, or any other shape can employ as a radiating patch [8]. A multi-band antenna is necessary to

reduce complexity and simplify the structure. Some studies have used triple-band antennas implemented using hexagonal shape and H-shape slots with cuts [9].

The antenna area can be scaled down. Multiband features are also achieved by counting meander lines on a four-sided strip ring [10]. A wideband antenna or ultra-wideband (UWB) with slots can also be used to generate numerous operational bands, resulting in dual-band or triple-band antennas. The width, length, and position of these gaps are generally affected by the working BWs and frequencies (f). Furthermore, the responses of the required bands substantially influence one another. Therefore, it is difficult to get the anticipated BWs and frequencies. The last approach for producing triple bands is to use a specialized antenna with a patch [11].

This paper presents a multiband slotted hexagonal antenna with a developed design. Multiband antenna design is made easier with the proposed structure and design approach. A simple and sequential method was utilized to obtain multiple bands while the structure was still in the same shape. This multi-band antenna is designed for WLAN, WiMAX, and LTE applications.

2. Antenna Design

Three sequential steps were taken in designing the suggested antenna to enable complete optional control and prevent errors. These processes entail laying a foundation structure for the main shape of the antenna first, then developing it theoretically and finally altering the dimensions to get the desired results.

2.1. Basic Structure

The basic structure for the planar antenna was modelled and evaluated to suit the desired target. The basic structure for the proposed antenna was of a hexagonal ring of a certain width, as the patch (made of copper) placed on a ground plane. Fig. 1 shows four views of the basic design of the proposed hexagonal antenna. Fig. 1a shows a 3-dimensional schematic diagram of the patch, substrate, and ground parts with unreal distances.

Basic measurements of the patch were determined through two radii (R_1 and R_2) of the circumscribed circle, as shown in Fig. 1b. The antenna was etched on a 1.6 mm thick flame retardant-4 (FR-4) substrate with relative permittivity (ϵ_r) of 4.4, and loss tangent ($\tan \delta$) of 0.02. Fig. 1c depicts a side view of the antenna with the essential dimensions, such as the copper patch thickness (h_c), which is approximately equal to 0.035 mm according to Printed Circuit Board (PCB) catalogues. Finally, the backside view in Fig. 1d represents the ground part of the antenna, which is all covered with a copper surface of the same thickness as the patch. The dimensions of the proposed antenna were calculated at the resonant frequency (f_r) of 2.4 GHz using MATLAB Software.

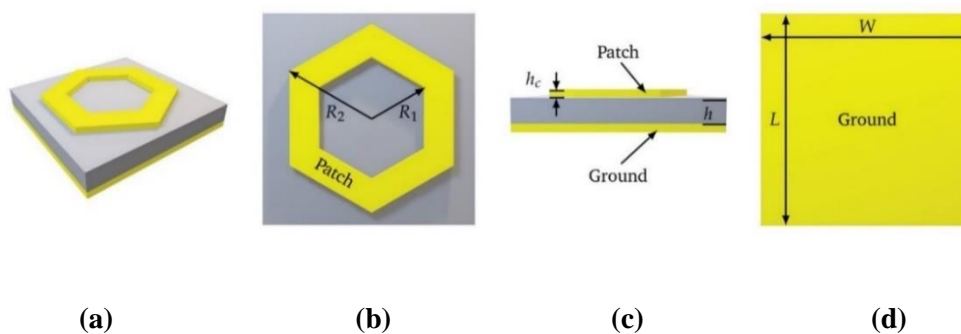


Figure 1: The base structure of proposed hexagonal antenna. (a) 3D View, (b) Front View, (c) Side View, (d) Back View.

2.2. Antenna Design Development

Several improvement steps were made to enhance the performance of the proposed hexagonal-shaped antenna with a clear multiband. Computer simulation technology (CST) was used to design and simulate the proposed antenna. An inset feed was employed as a transmission line because of its ease of control. Fig. 2a represents the main patch shape of the basic hexagonal ring form and the transmutation line without any additions or removals. Five changes were made on the patch: the first was by cutting a thin slit on the top vertex of the hexagonal ring, as shown in Fig. 2b. The second, as shown in Fig. 2c, another slit was cut on the opposite vertex of the hexagonal ring. The other changes are shown in Fig. 2 (d, e, and f), which illustrate the positions of the other slits.

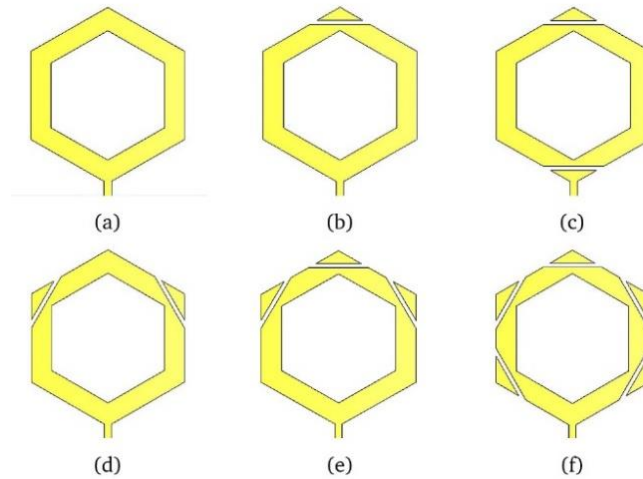


Figure 2: The model of proposed antenna evolution.

The length of the patch (L) and the width (W) were calculated according to equations 1 to 5 [12]:

$$W = \frac{c}{2f_r} \sqrt{\frac{2}{\epsilon_r + 1}} \quad (1)$$

$$L = L_{\text{eff}} - 2\Delta L \quad (2)$$

$$L_{\text{eff}} = \frac{c}{2f_r \sqrt{\epsilon_{\text{reff}}}} \quad (3)$$

$$\epsilon_{\text{reff}} = \frac{\epsilon_r + 1}{2} + \frac{\epsilon_r - 1}{2} \left[1 + 12 \frac{h}{W} \right]^{-1/2} \quad (4)$$

$$\Delta L = h \times 0.412 \frac{(\epsilon_{\text{reff}} + 0.3) \left(\frac{W}{h} + 0.264 \right)}{(\epsilon_{\text{reff}} - 0.258) \left(\frac{W}{h} + 0.8 \right)} \quad (5)$$

where (c) is the speed of light in vacuum taken as 299 792 458 m/s, (f_r) is the resonant frequency, (ϵ_{reff}) is effective dielectric constant, (L_{eff}) is effective length, and (ΔL) is extended length [12].

2.3. Geometrical of Optimum Antenna Design

Fig. 3 shows all the dimensions of the designed antenna, such as the substrate length (L), the substrate width (W), the inner circumscribed radius of the patch (R_1), the outer circumscribed radius of the patch (R_2), the slit start radius (R_3), the transmission line width (T_1), and the slit width (T_2).

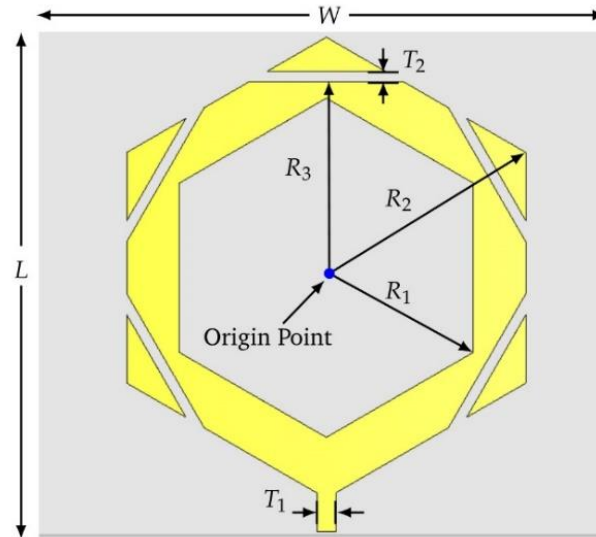


Figure 3: Structure of the proposed hexagonal antenna.

Table 1 lists the dimensions that were adopted in the proposed design. All magnitudes were rounded to one digit for practical reason as it is hard to implement micrometre dimensions.

Table 1: Proposed antenna variables and their values

Parameters	Dimensions (mm)
W	100
L	100
R_1	32.9
R_2	42.9
R_3	35.2
T_1	3.6
T_2	2

3. Simulation Results

Table 2 and Fig. 4 represent the reflection coefficient S_{11} vs operation frequencies of the six designs of the proposed hexagonal antenna. The results of the first three designs (of Fig. 2a, b and c) of the antenna are shown in Fig. 4a. The first design (Fig. 2a) operated on multiband frequencies, with the best value of s-parameter of -37.5 dB at 3.91 GHz of operation frequency. For the second design (Fig. 2b), the values of s-parameters became -22.55 dB and -28.4 dB at 4.05 GHz and 4.8 GHz, respectively, which represent the best results of this design. The third design of the antenna (Fig. 2c) had no results, because the current could not pass through the first slot.

Table 2: All operation regions and their S_{11} values of the suggested antennas in Fig. 2.

Return Loss	1st band		2nd band		3rd band		4th band		5th band		6th band	
	f_r (GHz)	S_{11} (dB)										
Fig (a)	2.74	-13.9	3.39	-13.7	3.91	-37.5	4.68	-15.7	5.2	-19.8	5.51	-15.4
Fig (b)	2.85	-13.5	3.53	-11.8	4.05	-22.55	4.8	-28.4	5.43	-13.8	---	---
Fig (c)	---	---	---	---	---	---	---	---	---	---	---	---
Fig (d)	2.73	-34.8	4.155	-29.4	4.77	-13.5	5.38	-11.9	---	---	---	---
Fig (e)	2.97	-35.3	4.28	-27.9	5	-29.75	---	---	---	---	---	---
Fig (f)	2.93	-14.73	3.64	-35.11	4.53	-14.2	5.08	-16.12	5.7	-18.4	---	---

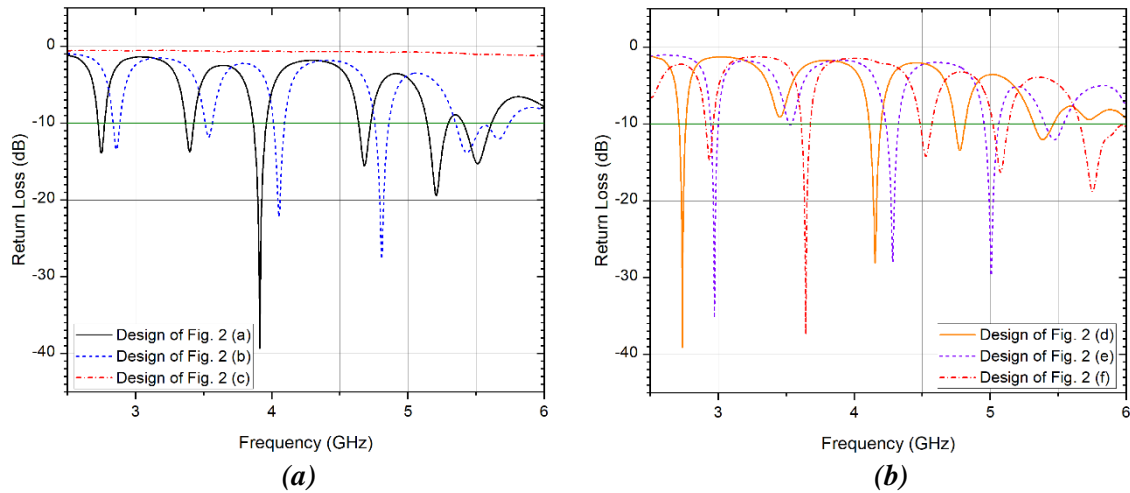


Figure 4: The simulation S_{11} of all proposed hexagonal antennas designs (a) the first three designs (b) the last three designs.

The results of the other three designs (of Fig. 2d, e and f) of the antenna are shown in Fig. 4b. The best values of the s-parameter were -34.8 dB at 2.73 GHz and -35.1 dB at 3.67 GHz for the designs of Fig. 2d and Fig. 2f, respectively. Finally, the fifth design of the proposed antenna (Fig. 2e) was chosen as the best design because of its ability to work at three useful operation frequencies with good results. These values are -35.3 dB at 2.97 GHz, -27.9 dB at 4.28 GHz, and -29.75 dB at 5 GHz, which are close to those employed in WLAN, WiMAX, and LTE applications.

3.1. Surface Current Distributions

Fig. 5 depicts the simulated surface current distributions of all the proposed antenna designs shown in Fig. 2. These surface currents, represented by small arrows, were calculated theoretically using CST software at a frequency of 2.4 GHz. The drawn arrows show the direction and intensity of the current flow on the surface of the copper patch. The colour difference in the colour depends on the current intensity, represented in units of decibels (A/m). The values of these colours are determined or indicated through the coloured ramp.

Fig. 5a show a fairly coordinated spread of the surface current as the patch was with no slits. But when one slit was cut in the copper patch, a narrow region was formed in the surface, which caused a delay in the passage of charges through it, and this, in turn, led to an increase in the distances between the current pulses, as shown in Fig.5b. Fig. 5c shows that there was no current on the surface of the patch and the reason is that the slit location was immediately after the feed line, which completely prevented the current from crossing. The distribution of slits in Fig. 5d had changed.

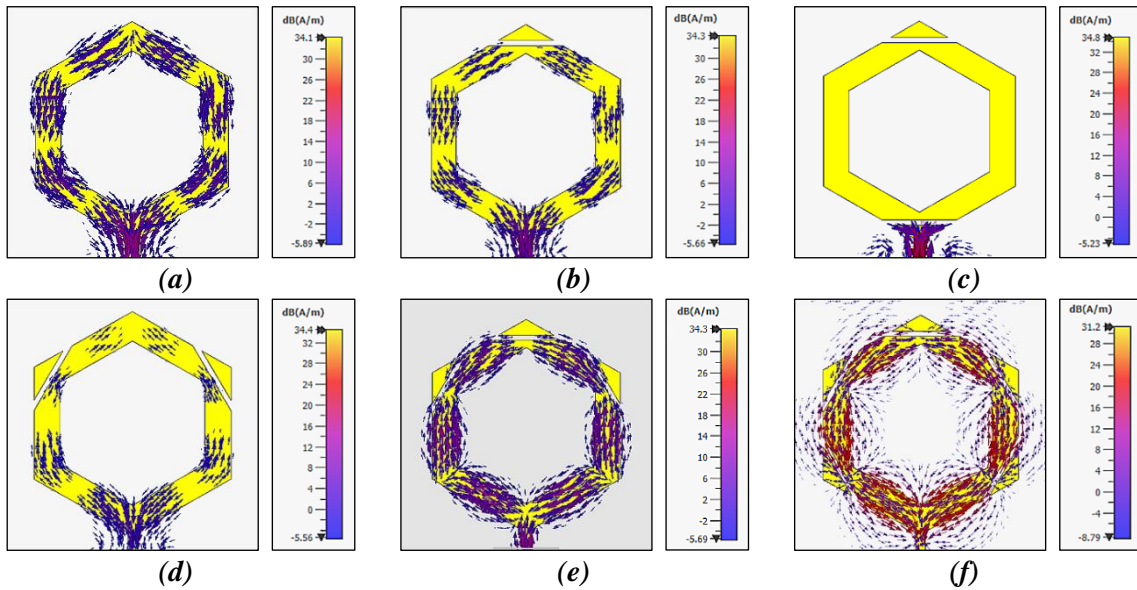


Figure 5: Surface current distributions on the surfaces of all proposed hexagonal antenna designs.

3.2. Electric Field Distributions

The electric field distributions on the hexagonal patch of the different designs of the antenna (shown in Fig. 2) at 2.4 GHz are shown in Fig. 6. The electric field distributions on the hexagonal patches of the proposed antennas of Fig. 2 (e and c) had the highest and lowest values, respectively.

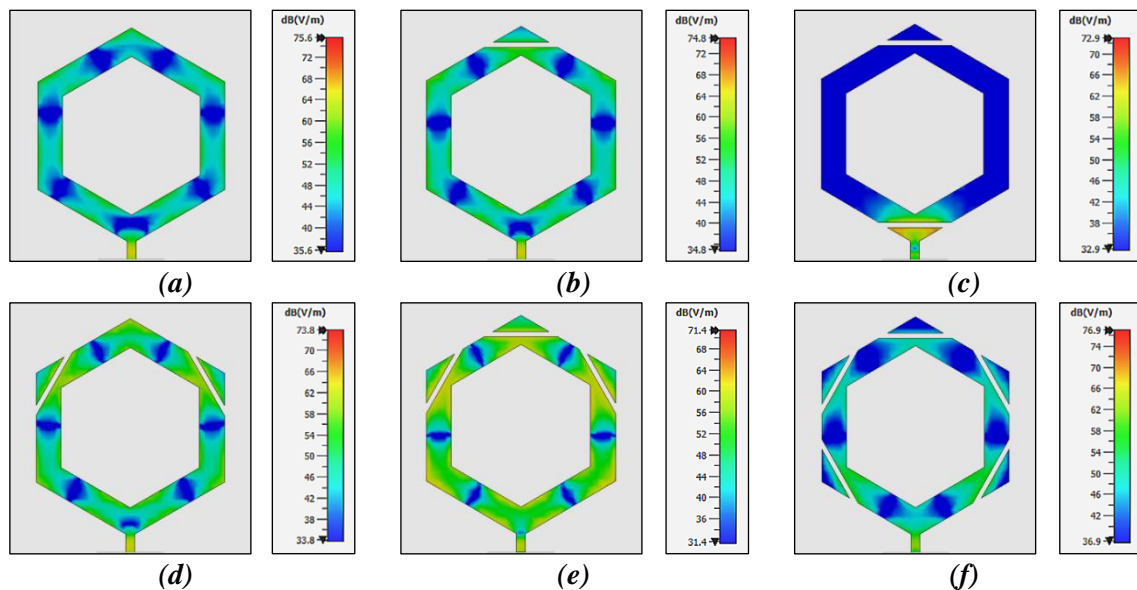


Figure 6: Simulated e-field distributions on all suggested antennas geometries' surfaces.

3.3. Radiation Patterns

The simulated patterns of the fifth design (Fig. 2e) are presented in Fig. 7. These three types of radiation have frequencies of 2.97 GHz, 4.28 GHz, and 5.47 GHz.

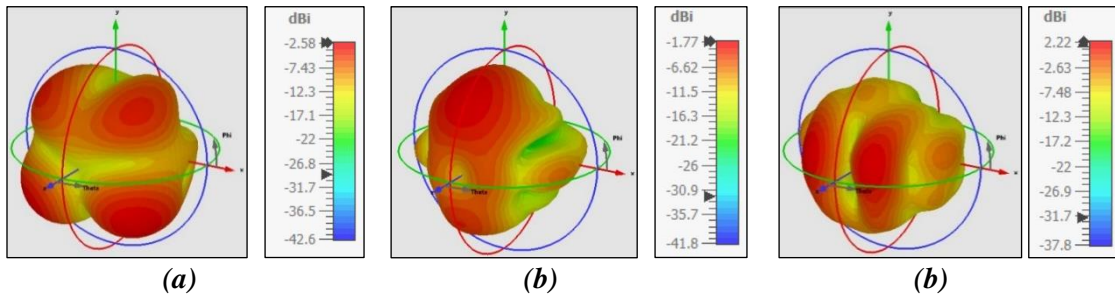


Figure 7: 3D radiation patterns of the fifth proposed design, (a) at the 2.97 GHz, (b) at the 4.28 GHz, (c) at the 5.47 GHz

3.4. Equivalent Circuit

The equivalent circuit of the antenna design in Fig. 2e can be illustrated in Fig. 8. Each slot is equivalent to an analogous equivalent admittance with conductance and susceptivity.

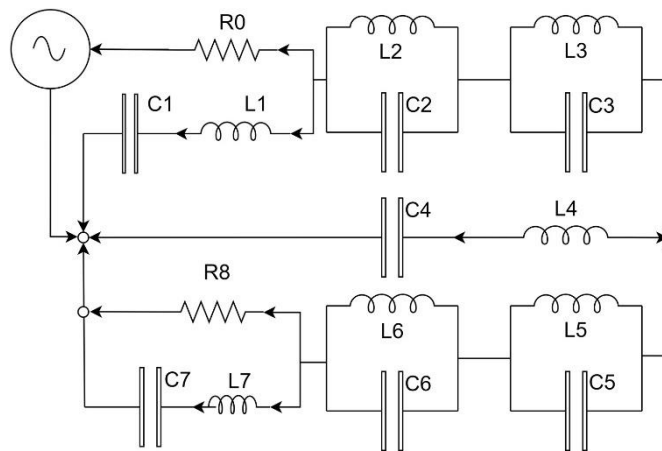


Figure 8: Equivalent circuit of the fifth model design.

4. Experimental Results

The hexagonal-MPA design (the fifth design of the proposed antenna, Fig. 2e) was fabricated on FR-4, as illustrated in Fig. 9.

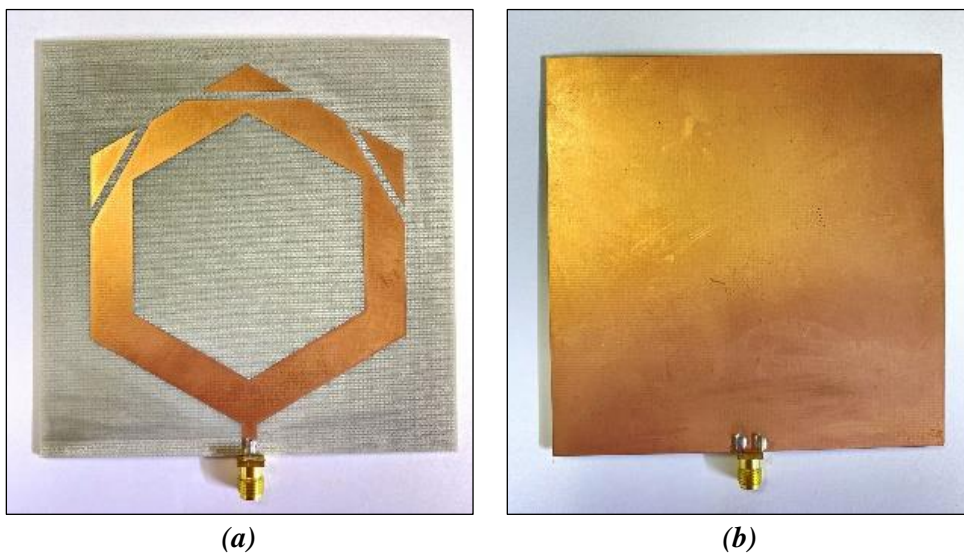


Figure 9: Manufactured form of the 5th proposed design of hexagonal -MPA, (a) Front view (b) Back view.

The PCB substrate thickness (h) was 1.33 mm, the dielectric constant (ϵ_r) was 4.424, and the copper plate thickness was 25 μm . The end launch jack holder was a Sub-Miniature Version A (SMA connector) with 50 ohms' impedance. It was fabricated using the computer numerical control (CNC) technique machine (Acctek AKM6090). After being manufactured, the antenna was tested experimentally using an ENA Series Network Analyser (E5071C, Agilent company) with a range from 300 kHz up to 20 GHz, as presented in Fig. 10.

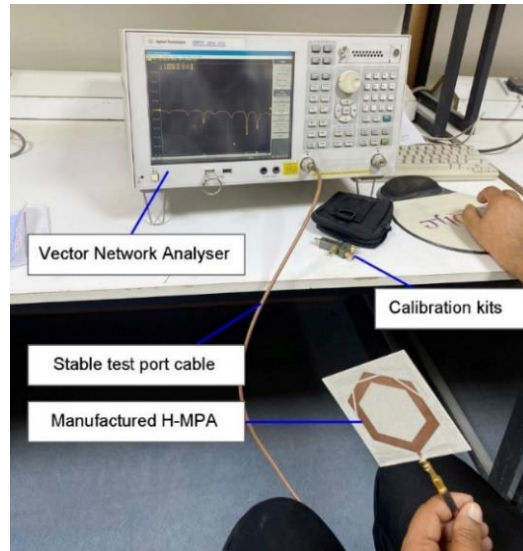


Figure 10: Testing process using an ENA series network analyser (E5071C).

5. Comparison

The comparison was made to detect changes in the results and study the causes. Two types of comparison are represented in this paper: the first is between the simulated and experimental results, and the second is between the practical results of this work and those of other studies.

5.1. Comparison Between Results

Fig. 11 represents the comparison between the simulated and the experimental results of the return loss as a function of frequency. The first apparent difference is that all the resonant frequencies in the experimental results have been slightly shifted to the left by approximately 0.1 GHz.

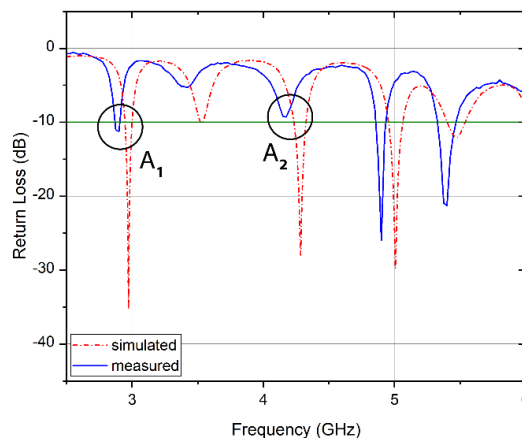


Figure 11: The comparison between the simulated and the experimental results of the return loss (RL).

The reason is that the thickness of the substrate used in the implementation process slightly differed from what was assumed in the simulation program. The second reason is that in the simulated work, the measurement accuracy was higher (1525 picks of the return loss for the selected range, which was from 1 GHz to 6 GHz), while that of the experimental was (201 picks for the same frequency range). This explanation shows why the values of the s-parameter did not appear in the marked areas A1 and A2 in Fig. 11. Table 3 shows the stimulated and experimental values of frequencies, return losses, and the bandwidth of the points indicated in Fig. 11. Generally, a decrease in the s-parameter values of the antenna can be observed in the frequency bands of 2.9 GHz and 4.17 GHz and, conversely, an increase in s-parameters at 4.9 GHz and 5.4 GHz of operation frequencies.

Table 3: Comparison between theoretical and measured results for four bands of the proposed antenna.

Bands	Simulation Results			Measurement Results		
	Fr (GHz)	RL (dB)	BW (MHz)	Fr (GHz)	RL (dB)	BW (MHz)
1st	2.97	-35.29	55.77	2.9	-11.24	32.0
2nd	4.28	-27.98	91.86	4.17	-9.31	---
3rd	5.00	-29.75	108.27	4.9	-25.99	75.0
4th	5.47	-12	130	5.4	-21.26	150.0

In addition, the practical results of the Voltage Standing Wave Ratio (VSWR) parameter values become 1.58, 1.67, 1.38, and 2.38 at 2.9 GHz, 4.15 GHz, 4.88 GHz, and 5.38 GHz of operation frequencies, respectively.

5.2. Comparisons with other Studies

The measured results of the suggested hexagonal antenna were compared to those of multi-band antennas of other studies, as shown in Table 4. For all antenna bands, emphasis is given on operating frequencies, return losses, and bandwidth. The first band operates at 4.9 GHz with 75 MHz of BW (from 4.85 GHz to 4.925 GHz). The second one operates at 5.4 GHz with 150 MHz of BW (from 5.325 GHz to 5.475 GHz).

Table 4: Parameters comparison of the antennas.

Ref.	Fr (GHz)	S11 (dB)	BW (MHz)	Gain(dBi)
Desai et al. [3]	3.79	-25.02	5500	6.5
	5.5	-26.03	5500	---
Benkhadda et al. [7]	3.6	-42.70	4350	2.78
	5.3	-50.06	4350	5.32
Cheng and Liu [13]	2.45	-27.00	380	7.3
	3.50	-15.00	380	6
Thi et al. [14]	3.1	-20	---	3.41
	5	-25	---	6.29
Mahatthanajatuphat et al. [15]	4.46	-32	1600	3
	5.56	-27	1600	2
This Work	4.9	-25.99	75	-1.76
	5.4	-21.26	150	2.26

6. Conclusions

After comparing the six theoretical results with each other, fifth design was chosen as the best to make a prototype. From the results, it is clear that the arrangement of the slits on the surface of the patch helped to create the soft movement of the current pulse and, in turn, led to the desired result. Studying and analysing the theoretical

results showed its efficiency in determining the best model among the proposed models before manufacturing. The narrow bands of the antenna helped it to not respond to unwanted frequencies. The fifth change of the proposed antenna (as illustrated in Fig. 2e) was chosen as the best design because of its ability to work at three useful operation frequencies with good results. These are -35.3 dB at 2.97 GHz, -27.9 dB at 4.28 GHz, and -29.75 dB at 5 GHz, which are so close to those employed in WLAN, WiMAX, and LTE applications. There are two measured bands that are below the level of 20 dB of the return loss which shows that the antenna operates at the lowest amount of power loss. In the future, the current antenna can be developed as a matrix antenna to increase efficiency and gain in these three operational regions. The proposed antenna is suitable for use in wireless systems such as universal mobile communications systems, WLAN, and RFID.

Acknowledgements

The authors would like to thank E-Solutions office - Baghdad - Iraq for manufacturing the antenna using the CNC method with good accuracy.

Conflict of interest

Authors declare that they have no conflict of interest.

References

1. Y. Huang and K. Boyle, *Antennas: from Theory to Practice*. (UK, John Wiley & Sons, 2021).
2. N. Sharma, S. S. Bhatia, V. Sharma, and J. S. Sivia, *Wirel. Personal Commun.* **111**, 1977 (2020).
3. A. Desai, T. K. Upadhyaya, R. Patel, S. Bhatt, and P. Mankodi, *Prog. Electromag. Res. Lett.* **74**, 125 (2018).
4. A. M. Abdulhussein, A. H. Khidhir, and A. A. Naser, *Int. J. of Microwave Optic. Tech.* **16**, 355 (2021).
5. R. A. Pandhare, P. L. Zade, and M. P. Abegaonkar, *Eng. Sci. Tech. Inter. J.* **19**, 1360 (2016).
6. N. L. Nhlengethwa and P. Kumar, *Inter. J. Smart Sens. Intel. Syst.* **14**, 1 (2021).
7. O. Benkhadda, S. Ahmad, M. Saih, K. Chaji, A. Reha, A. Ghaffar, S. Khan, M. Alibakhshikenari, and E. Limiti, *Appl. Sci.* **12**, 1142 (2022).
8. A. M. Abdulhussein, A. H. Khidhi, and A. A. Naser, *J. Phys.: Conference Series* (IOP Publishing, 2021). p. 012051.
9. M. Gupta and V. Mathur, *Turk. J. Elec. Eng. Comp. Sci.* **25**, 4474 (2017).
10. B. S. Taha and H. M. Marhoon, *Int. J. Adv. Appl. Sci.* **10**, 70 (2021).
11. A. Pirooj, M. Naser-Moghadasi, F. B. Zarrabi, and A. Sharifi, *Prog. Electrom. Res. C* **71**, 69 (2017).
12. C. A. Balanis, *Antenna Theory: Analysis and Design*. 4th Ed. (Hoboken, New Jersey, John Wiley & Sons, 2016).
13. Y. Cheng, H. Liu, and N. Nasimuddin, *Inter. J. Anten. Prop.* **2018**, 7560567 (2018).
14. T. N. Thi, S. Trinh-Van, G. Kwon, and K. C. Hwang, *Prog. Electrom. Res.* **143**, 207 (2013).
15. C. Mahatthanajatuphat, S. Saleekaw, P. Akkaraekthalin, and M. Krairiksh, *Prog. Electrom. Res.* **89**, 57 (2009).

تصميم وتحليل هوائي سداسي الشكل المزود بميزة النطاقات المتعددة لتطبيقات WLAN و LTE و WiMAX

علاء محمد عبد الحسين¹، وسن عبد الرحيم خلف²، نور الهدى محمد عبد الحسين³، ايمان ابراهيم عوض⁴، علي محمد علي⁴

¹قسم البعثات والعلاقات الثقافية، جامعة كربلاء، كربلاء، العراق

²قسم الفيزياء، كلية العلوم للبنات، جامعة بغداد، بغداد، العراق

³كلية الصيدلة، جامعة الزهراء للبنات، كربلاء، العراق

⁴قسم الفيزياء الطبية، كلية علوم الطب التطبيقية، جامعة كربلاء، كربلاء، العراق

الخلاصة

ان التطوير والبحث المستمر في تصميم الهوائيات يماثل التعدين في منجم غير مكتشف. في هذا البحث، تم اقتراح هوائي متعدد النطاقات بشكل حلقة سداسية جديدة، تم تصميمه وتطويره وتحليله نظرياً باستخدام برنامج CST قبل تصنيعه. لقد مر الهوائي بستة مراحل متتالية من أجل تحقيق أفضل النتائج المطلوبة. تم تحليل ودراسة النتائج في جانب توزيع التيار السطحي والمجال الكهربائي على سطح الرقعة السداسية نظرياً. الطريقة المتسلسلة التي تم استخدامها لتحديد التصميم الأكثر كفاءة هي منطقية، وقد ساهمت هذه الطريقة في منع الانحراف عن مسار العمل المقصود. بعد مقارنة النتائج الستة النظرية مع بعضها البعض تم اختيار التصميم الخامس لدخول مرحلة التصنيع. اظهرت النتائج المقاسة أن الهوائي المقترح يمكن أن يعمل بشكل جيد في ثلاث حزم مع خسارة عودة تبلغ 11.24 - ديسيبل عند 2.9 جيجا هرتز و 25.99 - ديسيبل عند 4.9 جيجا هرتز و 26.21 - ديسيبل عند 5.4 جيجا هرتز على التوالي. ينتمي هذا النوع من الهوائي إلى العديد من أنظمة الاتصالات اللاسلكية، بما في ذلك G2 و G3 و G4 و G5.

الكلمات المفتاحية: هوائيات مستوية، اتصالات، شكل سداسي، متعدد النطاقات، طريقة CNC.